Optics & Laser Technology 59 (2014) 110–115

Contents lists available at ScienceDirect

Optics & Laser Technology

journal homepage: www.elsevier.com/locate/optlastec

Effect of passivation layers on characteristics of AlGaInP ridge waveguide laser diodes

Chih-Tsang Hung, Shen-Che Huang, Tien-Chang Lu *

Department of Photonics & Institute of Electro-Optical Engineering, National Chiao Tung University, Hsinchu 30010, Taiwan

ARTICLE INFO

Article history:
Received 7 October 2013
Received in revised form
27 November 2013
Accepted 16 December 2013
Available online 9 January 2014

Keywords:
AlGaInP
Laser diodes
Dielectric layer

ABSTRACT

We investigate the effect of passivation structure on the optical mode distribution and characteristics of the edge emitting ridge waveguide AlGaInP–GaInP visible laser diodes (LDs). For conventional designs of single-layer Si_3N_4 or SiO_2 passivation, the variation of lateral near-field confinement and the horizontal far-field (FF) divergence can be determined via the modification of dielectric layer thickness. Thin passivation layer suffers from high absorption at the metal interface while thick passivation layer suffers from poor heat dissipation in the ridge waveguide and high scattering loss, resulting in high threshold. We propose a novel design of three-pair Al_2O_3/Ta_2O_5 multilayer optical thin films as passivation on the ridge waveguide, which can improve the laser characteristics and the heat dissipation. The measured room-temperature threshold current (*Ith*) and characteristic temperature (T_0) are 44.5 mA and 104.2 K with a divergence angle of 16.4°.

1. Introduction

High efficiency AlGaInP–GaInP visible laser diodes (LDs) are critical components for applications such as optical storage, laser display, distance measurement instrument, and photodynamic therapy for the therapy of cancer [1]. In order to achieve high performance operation, the typical AlGaInP LD structure utilized GaAs over-growth waveguide or narrow ridge strip design for lateral carrier and optical confinement [2]. However, these designs often lead to low quantum efficiency due to the optical absorption loss in the GaAs over-growth layers or extremely high facet power density due to the small emission area. Hence, it is hard to achieve high-power operation in the AlGaInP-based laser diodes. This can be addressed by the use of wider bandgap regrown materials, such as AlInP or AlGaInP, to construct an index guided laser structure [3,4]. Nonetheless, the design resulted in more complex crystal regrowth procedures and more defects occurring around the interface between these heterostructures. These defects would in turn increase the possibility of absorption and scattering loss, which gave rise to deterioration of the quantum efficiency. On the other hand, buried AlAs native oxides were proposed and adopted for carrier and optical confinement [5–7]. Although the design can improve the scattering loss and absorption around the edge of ridge waveguide, the high temperature treatment which would affect the operation stability of laser characteristics directly led to the change of doping profile in the epitaxial layers during the lateral wet oxidation.

In this paper we demonstrated a high-power AlGaInP–GaInP multi quantum wells (MQWs) LD with multi-layer thin films as passivation layers to modify the lateral optical mode distribution, which can be operated with a low threshold current density and high conversion efficiency with a single transverse mode operation. For a traditional ridge waveguide structure of the AlGaInP–GaInP red LDs, the single-layer dielectric thin film, such as SiO_2 or Si_3N_4 [8,9] often served as passivation layers. For the single-layer passivation processing, most researches paid attention to the adhesion around the interface and suppression of current leakage. Few reports focused on their influence on the *P–I* curve and optical confinement in the lateral transverse mode. Since the vertical divergence angle is determined by the refractive index guiding provided by the epitaxial layers, which is commonly larger than 20°, the horizontal divergence angle with values commonly ranging from 10° to 12° can be controlled by modifying the passivation layer on the ridge waveguide. Therefore, the structural modification of dielectric thin film could indeed play an essential role to modify the near-field (NF) optical mode distribution of edge emitting LDs to achieve a larger horizontal divergence angle and a smaller aspect ratio. To observe the effect of passivation layer modification on the characteristics of lateral optical field, we chose SiO_2 and Si_3N_4 dielectric thin films fabricated by plasma-enhanced chemical vapor deposition (PECVD) separately with several layer designs to deposit on the ridge waveguides of LDs. We further proposed multi-layer thin films to substitute the conventional

* Correspondence to: Department of Photonics, National Chiao Tung University, Advanced Nanophotonics and Semiconductor Laser Lab. No. 1001, Ta-Hsueh Rd., Hsinchu 30010, Taiwan. Tel.: +886 3 5712121x31234.
E-mail address: timtclu@mail.nctu.edu.tw (T.-C. Lu).

0030-3992/$ - see front matter
http://dx.doi.org/10.1016/j.optlastec.2013.12.014

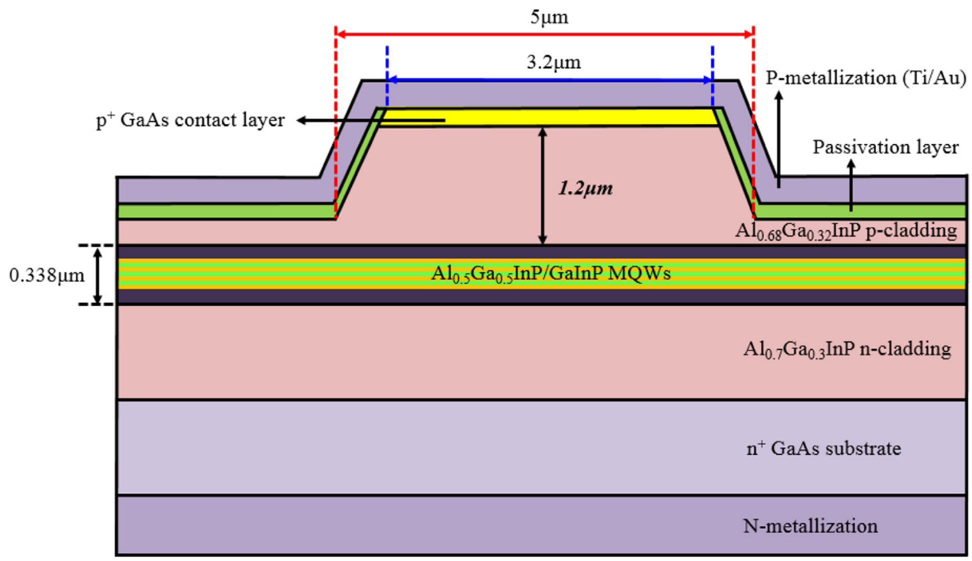

Fig. 1. The full structure of an AlGaInP–GaInP MQWs LDs containing a GaAs substrate, an n-type $Al_{0.7}Ga_{0.3}InP$ bottom cladding layer, AlGaInP–GaInP MQWs surrounded by two $Al_{0.5}Ga_{0.5}InP$ optical confinement layers followed by a p-type $Al_{0.68}Ga_{0.32}InP$ top cladding layer, and a p-type GaAs cap layer.

Table 1
The structural parameters of passivation layers [10,11].

No.	Material	Thickness [nm]
1	PECVD Si_3N_4	50
2		81
3		120
4		162
5		243
6		324
7		400
8	PECVD SiO_2	50
9		81
10		113
11		170
12		226
13		282
14		400
15	E-gun coating Al_2O_3/Ta_2O_5	537
16	E-gun coating SiO_2/TiO_2	558

structure of single-layer passivation. Utilizing the design with multi-layer passivation led to a better lateral confinement in the near-field distribution and higher conversion efficiency under high-power operation.

2. Experiment design and simulation

Schematics of AlGaInP–GaInP 650-nm edge-emitting laser diode are shown in Fig. 1. Epitaxial layers consisted of a GaAs substrate with high n-type doping, a 1.3 μm-thick n-type $Al_{0.7}Ga_{0.3}InP$ bottom cladding layer, an AlGaInP–GaInP active region, a p-type top cladding layer with an asymmetric $Al_{0.68}Ga_{0.32}InP$ composition, and a high level carbon doped GaAs cap layer. The active region containing two-pair strain-compensated GaInP–$Al_{0.5}Ga_{0.5}InP$ MQWs with a targeted thickness and composition to achieve the lasing wavelength of 650 nm was embedded in the separate confinement heterostucture (SCH) made from two 75-nm-thick $Al_{0.5}Ga_{0.5}InP$ layers. The stripe profile of ridge waveguide was set to be trapezoid-shape with 3.2 μm/5 μm for the top/bottom widths due to the wet etching process. We presented two types of passivation layers: single-layer and multi-layers designed structures which parameters are listed in Table 1. The multi-layer passivation included three-pair optical thin films with high and low refractive indices (Al_2O_3 101.6 nm/Ta_2O_5 77.4 nm, SiO_2 112.1 nm/TiO_2 73.8 nm). P/N-side metallization was set as Ti–Au and Ge–Au, respectively. The cavity length was chosen as 1000 μm. Modeling of the near-field optical mode profiles and laser diode characteristics was performed by using the two-dimensional optical mode solver coded by the transfer matrix method and the standard laser rate equations adopting reasonable material gain coefficients in the GaInP MQWs. The far-field output pattern was calculated by simple Fourier transform of the near-field optical profiles. We analyzed the far-field optical profiles in the horizontal direction by investigating the full width at half maximum (FWHM) of divergence angles, presented in Fig. 2.

First step, we observed the effect on the characteristics of optical field in the horizontal divergence for single-layer passivation cases of Si_3N_4 and SiO_2. Fig. 3(a) shows the calculated far-field FWHM of AlGaInP–GaInP LDs as a function of the thickness of dielectric layers. Comparing with the distribution of optical field in the LDs coated by the dielectric films with different thickness, the FF patterns possessed a broad horizontal divergence angle as the thickness was thinner than 100 nm. For the LDs which stripe covered with Si_3N_4 and SiO_2 50-nm-thick passivation, the far-field divergence angles can be obtained about 14.0° and 17.0°, respectively. If the dielectric film was deposited with much thinner thickness, some portion of the optical field would be absorbed by the titanium of *p*-metallization. The near-field optical mode in the lateral direction became narrower due to the edge waveguide absorption. In consequence, the far-field horizontal divergence became wider. If the dielectric thickness increased, the absorption effect can be reduced gradually and consequently the distribution of near-field lateral mode became broad simultaneously. The corresponding FF horizontal divergence angle can change to a smaller value. As the passivation thickness became much thicker than 120 nm, the FF mode profile would broaden again due to the better lateral optical confinement. The widest divergence beam can be obtained 16.3° and 17.9° respectively with 400-nm-thick Si_3N_4 and SiO_2 dielectric films. To sum up two series of samples coated by distinct dielectric layers, LDs covered with SiO_2 passivation can give rise to smaller far-field FWHM due to the lower refractive index of SiO_2 (n=1.45) than that of Si_3N_4 (n=2.05). On the other hand, the lateral optical confinement capability would become constant while further increasing the passivation layer thickness, such that the rising trend of FWHM became

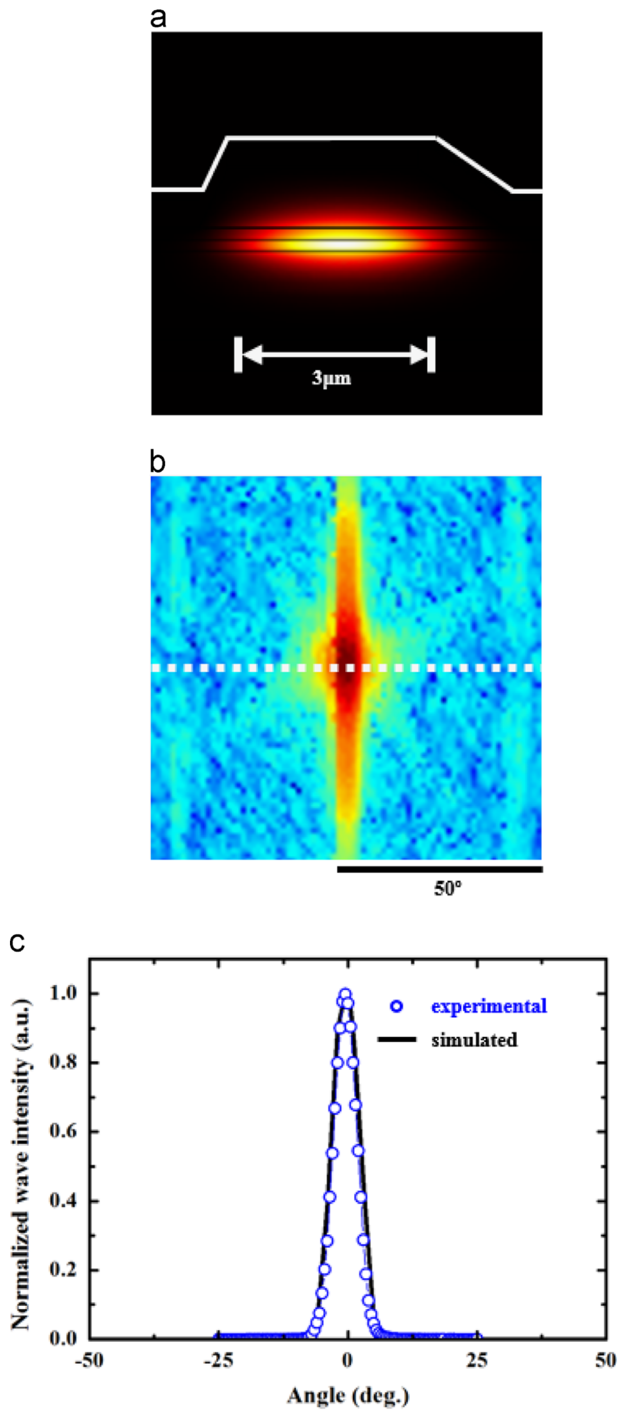

Fig. 2. (a) Calculated near-field optical mode distribution for the AlGaInP–GaInP LDs. (b) Far-field light pattern transformed from the near-field optical profile. (c) Intensity distribution of optical field in the horizontal far-field direction for the LD with 120-nm-thick silicon nitride.

saturated with passivation layer thickness close to the 400 nm. Therefore, according to the diagram of FWHM curves, an obvious valley point occurs and the minimum FWHM values of LDs covered with two dielectric films are 14.8° and 11.8°, respectively

As for the multi-layer passivation, we proposed two structures: three-pair Al_2O_3/Ta_2O_5 and SiO_2/TiO_2 DBR films to investigate the corresponding laser characteristics. The reflective index undulation in the multi-layer passivation could modulate the near field distribution in the ridge waveguide and thus enhance the optical confinement capability without introduction of optical loss at the

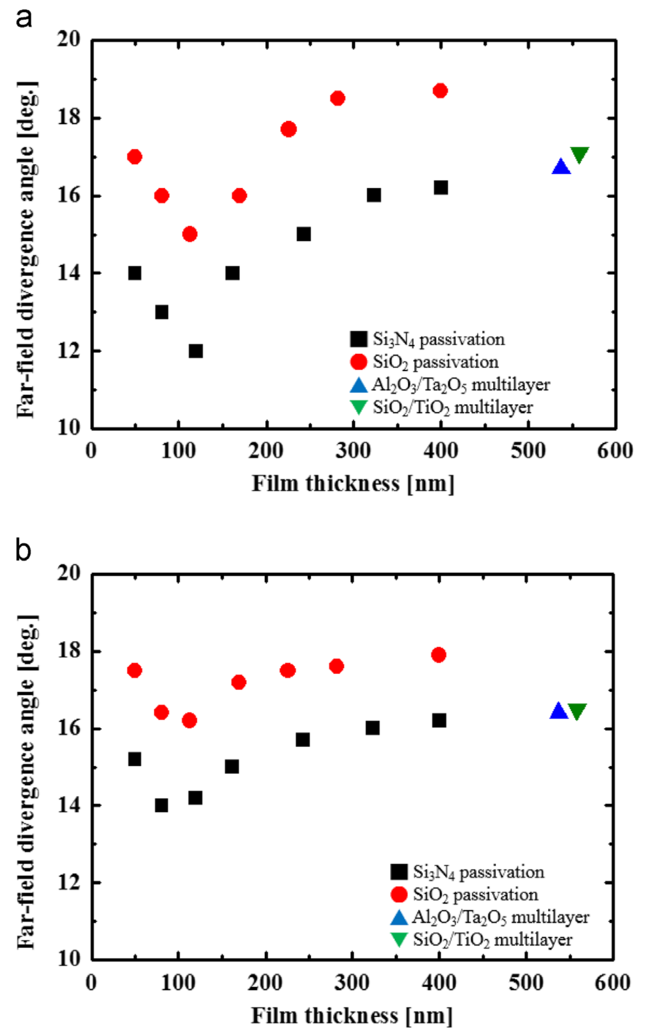

Fig. 3. (a) Simulated and (b) experimental far-field divergence angle measured at room temperature as a function of the thickness of passivation layers constituted by Si_3N_4, SiO_2 and multi-layer optical films.

metal interface. In addition, the multi-layer passivation could mitigate the structural strain occurred in the thick single passivation layer. The total thickness of two multilayers was 537 nm and 558 nm, which was thicker than above mentioned single-layer samples. Such thick passivation layer can efficiently diminish the power density around the emission end facet. The far-field FWHM of LDs coated with multilayers can still maintain within 17° even the total layer thickness was larger than 400 nm as shown in Fig. 3.

3. Results and discussion

According to the structure design of device modeling, we fabricated the AlGaInP–GaInP MQWs LDs in a low pressure metal-organic chemical vapor (MOCVD) system. All the epitaxial layers were grown on (1 0 0) n-type GaAs substrates with Si as the n-type dopant, Zn as the p-type dopant in the cladding layers and C as the p-type dopant in the contact layer. Narrow stripe (top/bottom width = 3.2/5 μm) ridge waveguide laser structures were manufactured by chemical wet etching. On the basis of the above-mentioned conditions of passivation, we deposited the single-layer dielectric film of Si_3N_4, SiO_2, and multi-layer passivation by PECVD and electron beam (e-beam) evaporation after lateral ridge waveguide etching processing. The corresponding structural parameters are listed in Table 1. In order to prevent the facet from

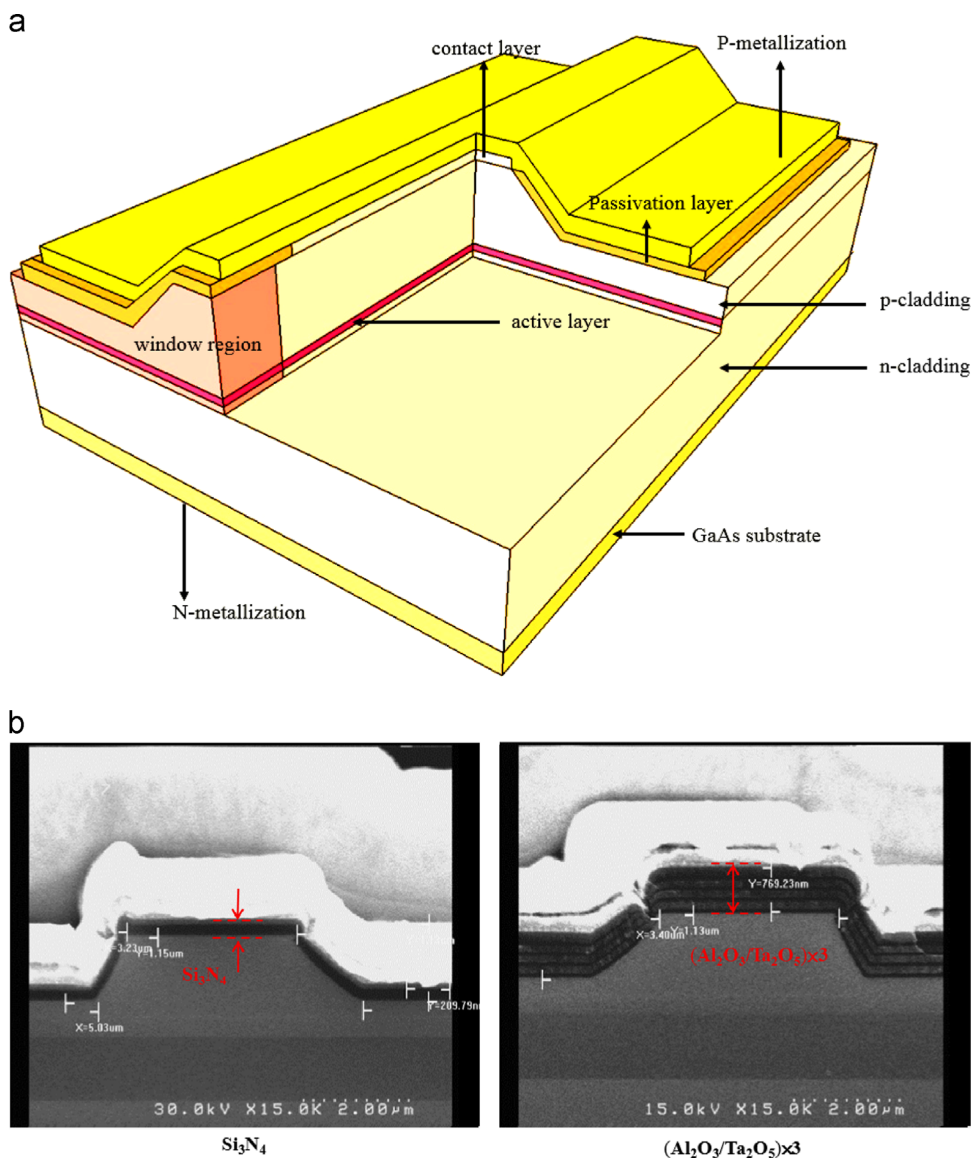

Fig. 4. (a) Schematic of the fabricated LD. The SEM cross section images of LDs covered with (b) Si_3N_4 dielectric layer and (c) 3-pair Al_2O_3/Ta_2O_5 multilayer.

catastrophic optical damage (COD) during high power operation, window mirror regions were made by using disordering of quantum wells with zinc diffusion. For selective current injection into a laser stripe, a GaAs contact layer was etched off and the passivation film was deposited at outside of a narrow stripe active area. Ti/Au and AuGe/Au metallization were applied as p-side and n-side contacts, respectively. Then, laser bars were cleaved and covered with antioxidant passivation so that the cavity length was 1000 μm. The facets were coated by e-beam evaporation with Al_2O_3/TiO_2 multilayers. These laser bars were tested on Cu heat sinks. A detailed schematic drawing of fabricated LD is shown in Fig. 4(a). Fig. 4(b) and (c) exhibits the cross sections of SEM images at the laser facet for LDs covered with the Si_3N_4 and three-pair Al_2O_3/Ta_2O_5 passivation, respectively.

Continuous wave (CW) characteristics of single-layer and multiple-layer types LDs were measured at operation temperatures of 25 °C, 40 °C, 50 °C, 60 °C, 70 °C and horizontal far-field patterns were taken by the corrected charge-coupled device (CCD) camera under the 120-mW operation power. It is worth noting that only fundamental transverse modes with no trace of higher order modes have been observed in the LDs, which are similar to the modeling results of the optical field distribution. First we again focused on the case of single-layer Si_3N_4 passivation, the strongly non-radiative absorption effect due to much thinner Si_3N_4 led to a narrower lateral near-field optical mode and then contributed to a wider far-field divergence pattern. Comparing to the modeling results, the influence of metal absorption was more serious in the actual experiments and hence the measured divergence angle exhibited a larger value (FWHM = 15.2°) with the 50-nm-thick passivation as shown in Fig. 3(b). As the thickness of passivation layer increased, the absorption effect would become weaker gradually and we can similarly obtain a valley point of FWHM curve located at approximately 100 nm (FWHM ~13.9°) of the Si_3N_4 passivation layer due to the broadening of lateral optical mode. As the passivation thickness became much thicker than 100 nm, the horizontal FF divergence angle rose from 13.9° to 16.2°. The main reason is that the thicker passivation layer provides a better lateral optical confinement, which attributes to a broadening effect on the horizontal far-field pattern. The investigation was similar to the calculated results and the increasing rate of divergence angle as a function of the passivation layer thickness became slowly and saturated when the thickness was close to the 400 nm thickness. The same trend of FWHM variation can also be obtained experimentally from the LDs coated by SiO_2

dielectric layers as shown in Fig. 3(b). A minimum value of FF divergence angle (FWHM = 16.2°) was occurred with the 113-nm-thick SiO_2 passivation. Comparing with Si_3N_4, the lower refractive index of SiO_2 under the same thickness of passivation layers fabricated by PECVD resulted in the wider far-field FWHM. In order to further avoid the absorption from the Ti–Au metallization, utilizing the high/low refractive-index composition multiple-layer passivation can modulate the near field distribution and apparently provided good optical mode confinement capability. In addition, the power density around the laser emitting facet could be reduced. The measured far-field divergence angles for the Al_2O_3/Ta_2O_5 and SiO_2/TiO_2 multiple-layer passivation structures were 16.4° and 16.5° respectively.

The variations of threshold current (Ith) and characteristic temperature as a function of passivation thickness operating at room-temperature are plotted in Fig. 5. As we mentioned before, the thinner passivation would suffer from absorption at the metal interface leading to the high threshold current Ith during high-power operation. We can observe from Fig. 5(a) that no matter what the single-layer passivation is, the threshold current tendency as a function of the passivation film thickness is quite similar to the far-field divergence. It is interesting to see that as the passivation layer became much thicker enough, the threshold current soon rose substantially. This could be due to the more residual heat accumulating during high-power operation when the passivation layer was too thick. In addition, the scattering loss would become prominent when the single passivation layer gets thicker, which could be due to the accumulated strain in the thick dielectric layer. The accumulated thermal energy could lead to the electron overflow from the MQWs region and then carrier injection efficiency would become lower, especially under high-temperature or high-power CW operation. This phenomenon can also be testified by the comparison that the threshold current of the LDs coated with SiO_2 is higher than Si_3N_4 case under the same film thickness, which could be due to the worse thermal conductivity of SiO_2. For Si_3N_4 and SiO_2 fabricated by PECVD, the measured values of thermal conductivity are 1.1 W/m-K and 16 W/m-K, respectively. Figs. 6 and 7 show the room temperature CW L-I characteristics of ridge waveguide LDs covered with single-layer and multi-layer passivation. It can be clearly seen that the Si_3N_4 layer shows not only lower experimental threshold current but also better slope efficiency under several film thicknesses in comparison to the SiO_2 case as shown in Fig. 6.

The characteristic temperatures are defined using T_0 that are the measures of temperature sensitivity to the threshold current, expressed as $I\text{th} = I\text{th}(0)\exp(\Delta T/T_0)$, where Ith(0) and Ith are threshold currents before and after changing the operation temperature, and ΔT is the variation of temperature. Driving working temperature form 25 °C to 70 °C, either Si_3N_4 or SiO_2 single-layer passivation showed the same characteristic temperatures tendency as shown in Fig. 5(b). We attributed the T_0 drop more obviously to more residual heat under a thicker dielectric film beyond 80 nm. The maximum characteristic temperatures

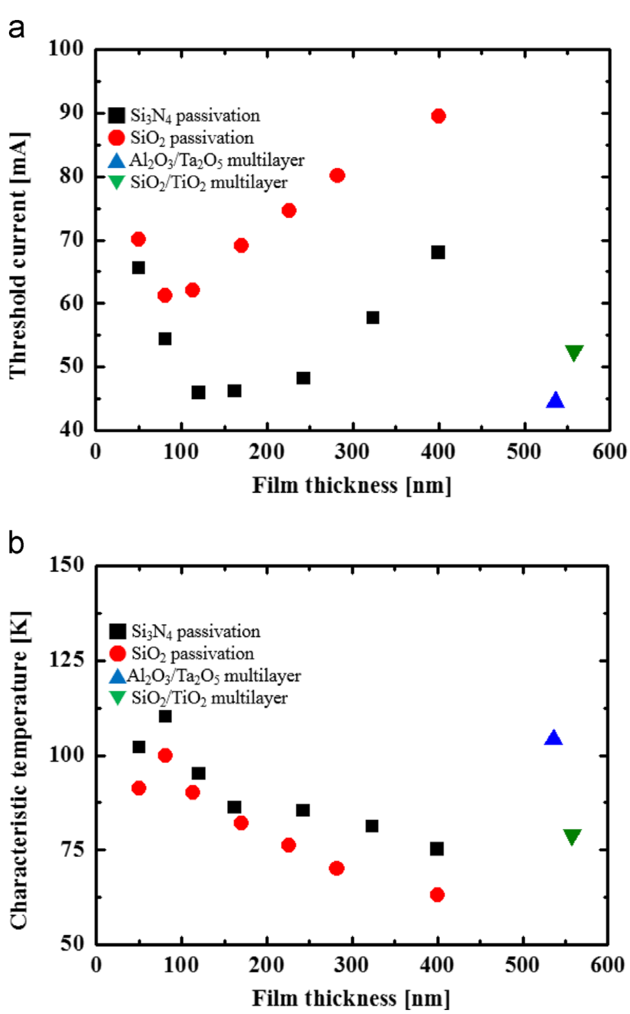

Fig. 5. The threshold current and characteristic temperature as a function of the thickness of passivation layers constituted by Si_3N_4, SiO_2 and multi-layer optical films.

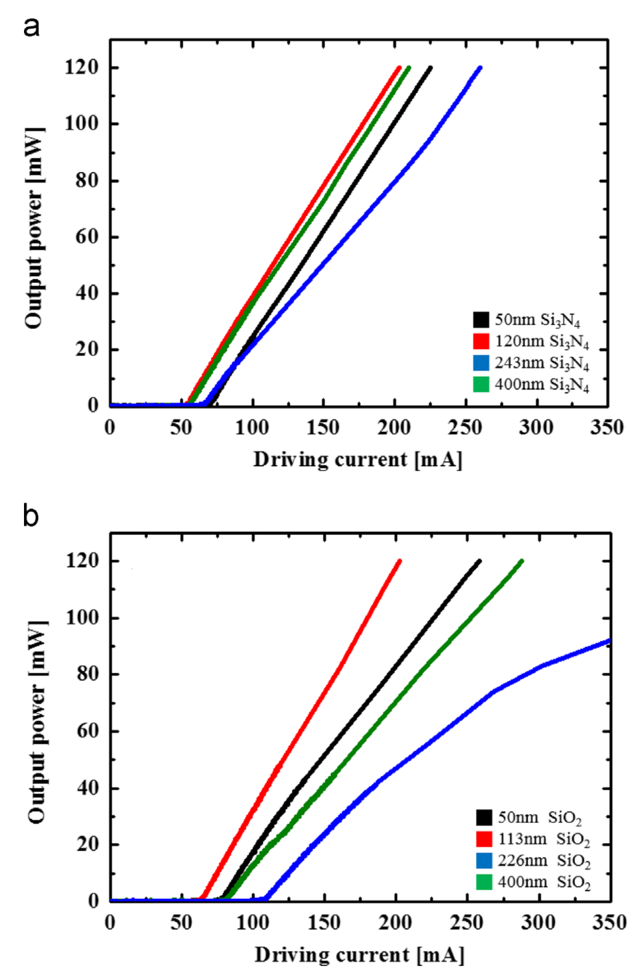

Fig. 6. The influence of passivation thickness on the room temperature CW L-I characteristics of ridge waveguide LDs covered with (a) Si_3N_4 and (b) SiO_2 dielectric layers.

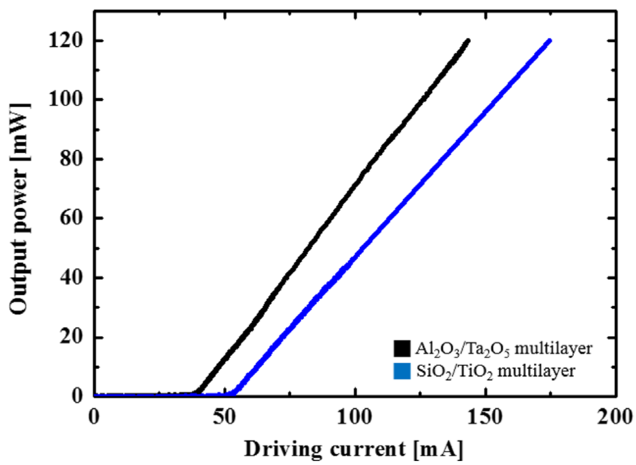

Fig. 7. The room temperature CW L-I characteristics of LDs coated with Al_2O_3/Ta_2O_5 and SiO_2/TiO_2 multi-layer passivation.

were 110.2 K and 99.8 K for the 81-nm-thick Si_3N_4 and SiO_2, respectively.

Similarly, the LDs with multi-layer optical thin films as passivation still possessed relatively low threshold current. As shown in Fig. 7, the room-temperature threshold currents are 44.5 mA and 52.6 mA for Al_2O_3/Ta_2O_5 and SiO_2/TiO_2 multilayers respectively. The multi-layer structure could efficiently reduce the scattering effect, which could be due to the less accumulating strain. Thus the light can be confined within the ridge stripe to enhance the quantum efficiency which attribute to improvement of threshold current. Since the thermal conductivity of Al_2O_3/Ta_2O_5 was better than SiO_2/TiO_2, the threshold current of Al_2O_3/Ta_2O_5 passivation was smaller than the SiO_2/TiO_2 multilayer due to the better thermal conductivity. Furthermore, the characteristic temperature of Al_2O_3/Ta_2O_5 case was much better than SiO_2/TiO_2 multilayers (104.02 K > 79.06 K). As shown in Fig. 7, we have achieved a stable and kink-free high power operation (120 mW) for LDs with multi-layer Al_2O_3/Ta_2O_5 optical thin films due to the good heat-dissipation structure and good optical confinement capability.

4. Conclusions

We successfully developed high-power AlGaInP–GaInP MQWs ridge waveguide LDs with Al_2O_3/Ta_2O_5 multi-layer structures as passivation to obtain stable lateral optical mode distribution and optimized electrical characteristics, demonstrating low threshold current, high conversion efficiency and large horizontal divergence angle. Compared to the conventional design of single-layer passivation, the multilayer passivation presented much thicker thickness to avoid the metal absorption and improves the scattering loss, which decreased the threshold current and increased the conversion efficiency. Since the Al_2O_3/Ta_2O_5 multilayer possessed better temperature characteristics, the LDs became more proper at high-temperature operation. The measured room-temperature threshold current and characteristic temperature were 44.5 mA and 104.2 K without any power-kink with divergence angle of 16.4°.

Acknowledgement

This work was supported in part by the Ministry of Education Aim for the Top University program and by the National Science Council of Taiwan under Contract No. NSC 100-2628-E-009-013-MY3, and NSC 102-2221-E-009-156-MY3.

References

[1] Usuda J, Kato H, Okunaka T, Furukawa K, Tsutsui H, Yamada K, et al. Photodynamic therapy (PDT) for lung cancers. J Thorac Oncol 2006;1(5):489–93.
[2] Ishikawa M, Ohba Y, Watanabe Y, Nagasaki H, Sugawara H, Yamamoto M, et al. InGaAlP transverse mode stabilized visible laser diodes fabricated by MOCVD selective growth. In: Extended abstracts of the 18th international conference on solid state devices and materials. Tokyo, Japan; 1986. p. 153–6.
[3] Kobayashi R, Hotta H, Miyasaka F, Hara K, Kobayashi K. Real index-guided AlGaInP visible laser with high-bandgap energy AlInP current blocking layer grown by HCl-assisted metalorganic vapor phase epitaxy. IEEE J Sel Top Quantum Electron 1995;1(2):723–7.
[4] Lu TC, Shieh HM, Wang SC. Real index-guided InGaAlP red lasers with buried tunnel junctions. Appl Phys Lett 2002;80:1882–4.
[5] Maranowski SA, Sugg AR, Chen EI, Holonyak Jr. N. Native oxide top-and bottom confined narrow stripe p–n $Al_yGa_{1-y}As$–GaAs–$In_xGa_{1-x}As$ quantum well heterostructure laser. Appl Phys Lett 1993;63:1660.
[6] Cheng Y, Dapkus PD, MacDougal MH, Yang GM. Lasing characteristics of high-performance narrow-stripe InGaAs–GaAs quantum-well lasers confined by AlAs native oxide. IEEE Photonics Technol Lett 1996;8(2):176–8.
[7] Floyd PD, Sun D, Treat DW. Low-threshold laterally oxidized GaInP–AlGaInP quantum-well laser diodes. IEEE Photonics Technol Lett 1998;10(1):45–7.
[8] Bour DP, Beernink KJ, Treat DW. AlGaInP single quantum well laser diodes. SPIE Visible UV Lasers 1994;2115:269–80.
[9] Wood SA, Smowton PM, Molloy CH, Blood P, Somerford DJ, Button CC. Direct monitoring of thermally activated leakage current in AlGaInP laser diodes. Appl Phys Lett 1999;74:2540–2.
[10] Gorodetsky ML. Thermal noises and noise compensation in high reflection multilayer coating. Phys Lett A 2008;372(46):6813–22.
[11] Mun J, Kim SW, Kato R, Hatta I, Lee SH, Kang KH. Measurement of the thermal conductivity of TiO_2 thin films by using the thermo-reflectance method. Thermochim Acta 2007;455(1–2):55–9.